

# **SANDIA REPORT**

SAND2000-2654

Unlimited Release

Printed November 2000

## **Adiabatic Quasi-Spherical Compressions Driven by Magnetic Pressure for Inertial Confinement Fusion**

Thomas J. Nash

Prepared by  
Sandia National Laboratories  
Albuquerque, New Mexico 87185 and Livermore, California 94550

Sandia is a multiprogram laboratory operated by Sandia Corporation,  
a Lockheed Martin Company, for the United States Department of  
Energy under Contract DE-AC04-94AL85000.

Approved for public release; further dissemination unlimited.



**Sandia National Laboratories**

Issued by Sandia National Laboratories, operated for the United States  
Department of Energy by Sandia Corporation.

**NOTICE:** This report was prepared as an account of work sponsored by an agency of the United States Government. Neither the United States Government, nor any agency thereof, nor any of their employees, nor any of their contractors, subcontractors, or their employees, make any warranty, express or implied, or assume any legal liability or responsibility for the accuracy, completeness, or usefulness of any information, apparatus, product, or process disclosed, or represent that its use would not infringe privately owned rights. Reference herein to any specific commercial product, process, or service by trade name, trademark, manufacturer, or otherwise, does not necessarily constitute or imply its endorsement, recommendation, or favoring by the United States Government, any agency thereof, or any of their contractors or subcontractors. The views and opinions expressed herein do not necessarily state or reflect those of the United States Government, any agency thereof, or any of their contractors.

Printed in the United States of America. This report has been reproduced directly from the best available copy.

Available to DOE and DOE contractors from

U.S. Department of Energy  
Office of Scientific and Technical Information  
P.O. Box 62  
Oak Ridge, TN 37831

Telephone: (865)576-8401

Facsimile: (865)576-5728

E-Mail: [reports@adonis.osti.gov](mailto:reports@adonis.osti.gov)

Online ordering: <http://www.doe.gov/bridge>

Available to the public from

U.S. Department of Commerce  
National Technical Information Service  
5285 Port Royal Rd  
Springfield, VA 22161

Telephone: (800)553-6847

Facsimile: (703)605-6900

E-Mail: [orders@ntis.fedworld.gov](mailto:orders@ntis.fedworld.gov)

Online order: <http://www.ntis.gov/ordering.htm>



## **Adiabatic Quasi-Spherical Compressions Driven by Magnetic Pressure for Inertial Confinement Fusion**

Thomas J. Nash  
Diagnostics and Target Physics Department  
Sandia National Laboratories  
P.O. Box 5800  
Albuquerque, NM 87185-1196

### **Abstract**

The magnetic implosion of a high-Z quasi-spherical shell filled with DT fuel by the 20-MA Z accelerator can heat the fuel to near-ignition temperature. The attainable implosion velocity on Z, 13-cm/ $\mu$ s, is fast enough that thermal losses from the fuel to the shell are small. The high-Z shell traps radiation losses from the fuel, and the fuel reaches a high enough density to reabsorb the trapped radiation. The implosion is then nearly adiabatic. In this case the temperature of the fuel increases as the square of the convergence. The initial temperature of the fuel is set by the heating of an ion acoustic wave to be about 200-eV after a convergence of 4. To reach the ignition temperature of 5-keV an additional convergence of 5 is required. The implosion dynamics of the quasi-spherical implosion is modeled with the 2-D radiation hydrodynamic code LASNEX. LASNEX shows an 8-mm diameter quasi-spherical tungsten shell on Z driving 6-atmospheres of DT fuel nearly to ignition at 3.5-keV with a convergence of 20. The convergence is limited by mass flow along the surface of the quasi-spherical shell. With a convergence of 20 the final spot size is 400- $\mu$ m in diameter.

## Contents

I. Introduction .....	4
II. Adiabatic Quasi-Spherical Compressions .....	4
III. LASNEX inputs .....	5
IV. LASNEX outputs .....	6
V. Experimental Access.....	7
VI. High Yield.....	8
VII. Summary.....	8

## Figures

1. Diagram of Quasi-Spherical load for Z.....	10
2. 1D SCREAMER calculation of current and radius versus time for an 8-mm diameter 20 -mg load to 30 degrees latitude on Z.....	11
3. 1D SCREAMER calculation of velocity and kinetic energy versus time for an 8-mm diameter 20-mg load to 30 degrees latitude on Z.....	12
4. 1D SCREAMER calculation of radius and magnetic pressure versus time for an 8-mm diameter 20-mg load to 30 degrees latitude on Z.....	13
5. Skin depth of tungsten shell versus plasma temperature for a 100-ns pulse.....	14
6. Plasma temperature of tungsten shell versus shell depth for a 50- $\mu$ m skin depth on Z.....	15
7. Shell radius versus time from SCREAMER and from LASNEX.....	16
8. Average fuel temperature and outer radius versus time.....	17
9. Average fuel temperature versus fuel outer radius.....	18



# Adiabatic Quasi-spherical Compressions Driven by Magnetic Pressure for Inertial Confinement Fusion

## I. Introduction

The concept of an adiabatic quasi-spherical compression is well known in the field of magnetized target fusion (MTF). (1) In MTF the DT fuel is magnetized to limit thermal conductivity from the fuel to the imploding shell. Typical implosion velocities in MTF are 1-cm/ $\mu$ s. Such implosions have been done on SHIVA. (2)

On the pulsed-power driver Z (20-MA, 100-ns) it is possible to fabricate quasi-spherical loads that implode at 13-cm/ $\mu$ s. (3) This is fast enough that thermal losses do not prevent ignition. If the imploding quasi-spherical shell is a high Z material, such as gold or tungsten, the kinetic energy of implosion can be efficiently coupled to internal energy of the DT fuel, and the implosion is adiabatic. An adiabatic implosion efficiently couples the energy of pulsed-power drivers such as Z into internal energy of fusion fuel.

Other approaches to driving fusion with pulsed power include the dynamic hohlraum, (4,5,6), the Z-pinch driven hohlraum (7), and the static-wall hohlraum (8) concepts. In all of the above approaches radiation is used to drive an ICF pellet, and the pellet is designed for isentropic compressions. (9) In isentropic compressions shock waves do not outrun the implosion front. The waveform for the drive pressure in isentropic compressions is very sharply rising in time and very sensitive to the temporal profile of the drive temperature.

Quasi-spherical adiabatic compressions on pulsed-power drivers offer several advantages over isentropic ablatively driven compressions. The first advantage is efficiency. In the quasi-spherical implosion kinetic energy of implosion is converted directly into fuel internal energy. This is much more efficient than converting kinetic energy into radiation, and radiation back to kinetic energy again. The second advantage is insensitivity to drive shape. Because the implosion is not isentropic the waveform of the magnetic pressure may be used as the pulsed-power machine provides. A third advantage is that cryogenic fuel is not necessary. A fourth advantage is that the quasi-spherical shells are large, 8 mm on Z, therefore the ignition spots are large, hundreds of microns, and burn fractions are improved over smaller 2 mm diameter isentropic pellets.

## II. Adiabatic Quasi-spherical Compressions

In an adiabatic compression the kinetic energy of implosion of a shell is converted to internal energy of plasma fill. This can be realized on Z for high-Z shells such as tungsten compressing low Z gases such as DT fuel. In quasi-spherical implosions the change in load inductance is proportional to the shell radius. For a quasi-spherical implosion on Z with 20 MA to the load with the shell extending from -30 to +30 degrees latitude as shown in figure 1, the kinetic energy of the implosion is determined by the change of load inductance to be

$$K(kJ) = 400r_0 (cm) \quad (1)$$

where  $r_0$  is the initial radius of the quasi-spherical shell. The energy required to heat DT fuel to the ignition temperature of 5-keV is

$$E(kJ) = 600 m_f (mg) \quad (2)$$

where  $m_f$  is the mass of the DT fuel. Setting equation (1) equal to equation (2) gives the maximum mass of DT fuel that can be volumetrically ignited as

$$m_f (mg) < 0.67 r_0 (cm) \quad (3)$$

For a 4-mm radius quasi-spherical shell on Z the maximum amount of DT fuel that can be heated to ignition is then 270- $\mu$ g. In an adiabatic compression all of the PdV work done on the fill plasma is converted to plasma internal energy. For such a situation the fill plasma temperature T increases as the square of the convergence.

$$T = T_0 (r_0 / r)^2 \quad (4)$$

If the fuel is preheated by ion sound waves to 200-eV, a further convergence of 5 is necessary to heat the fuel to the ignition temperature of 5-keV.

In a quasi-spherical compression the magnetic pressure is greater at higher latitudes because the current is closer to the axis. To keep the acceleration constant along the shell, typically the shell thickness  $t$  varies with latitude as

$$t \propto (1 / \cos \theta)^2 \quad (5)$$

This is depicted schematically in figure 1, which shows a quasi-spherical shell appropriate for Z filled with 6-atmospheres of DT fuel. The shell extends from -30 degrees to +30 degrees latitude to minimize shell mass variation while still maintaining quasi-spherical compression. The tungsten shell is 8- $\mu$ m thick at the equator increasing to 10.5- $\mu$ m thick at 30 degrees latitude.

### III. LASNEX Inputs

The circuit code SCREAMER is used to model the implosion of the quasi-spherical shell shown in figure 1. The results are shown in figures 2 through 4, which depict the current, radius, velocity, kinetic energy, and magnetic pressure versus time. Peak current is 22 MA. The implosion time is 100 ns. The peak velocity is 12.5 cm/ $\mu$ s and the peak kinetic energy is 160 kJ. The mass of the tungsten shell is 20 mg, and the mass of the DT

fuel is 150  $\mu\text{g}$ . When the shell has reached a velocity of 10 cm/ $\mu\text{s}$  the magnetic pressure is less than 30 Mbar.

The magnetic pressure as shown in figure 4 is used as a source term for a two-dimensional LASNEX simulation. The pressure shown in figure 4 is the equatorial pressure. The pressure versus latitude varies as in equation 5, and this pressure variation with latitude is included in the source for the two-dimensional LASNEX simulation.

Figure 5 shows the skin depth versus shell temperature for a 100-ns pulse. (10) One can estimate the average temperature in the skin of the current-carrying shell by setting Spitzer heating equal to Planckian radiation loss.

$$T(\text{eV}) = 4.2(I(\text{MA}) / r_0(\text{cm}))^{.3636} (Z \ln \Lambda / \delta)^{.1818} \quad (6)$$

By setting the skin depth to 50- $\mu\text{m}$ , the shell radius to 0.4-cm, and the charge state to 8, one arrives at the average temperature in the skin to be 87-eV. Deeper into the shell than the skin depth one expects the temperature to drop. By approximating an exponential decay in the current one can arrive at a temperature variation across the shell.

This temperature variation is shown in figure 6 and is used as the initial temperature of the shell mass for the two-dimensional LASNEX runs. The initial density of the shell mass is set by uniformly distributing the mass over a 400- $\mu\text{m}$  thickness. One sees from figure 6 that the current will only heat the outermost portion of the plasma shell. The two-dimensional LASNEX simulation inputs then vary the shell mass as a function of latitude and the shell temperature as a function of radius.

#### IV. LASNEX Outputs

The implosion of the quasi-spherical shell of figure 1 in LASNEX closely matches the implosion of the shell in SCREAMER. This is indicated in figure 7, and shows that the pressure source in LASNEX is appropriately imploding the quasi-spherical shell.

With respect to the time scale of figures 2 through 4 the LASNEX run starts at 50-ns. The temperature inputs across the thickness of the shell as modeled in section III are consistent with the radiation transport included in LASNEX in that they persist for 25-ns in the LASNEX run until the shell starts to implode and a shock is launched through the shell. This occurs around 75-ns.

At 105-ns the shell has imploded from 0.4-cm radius to 0.3-cm radius. At this time the outside of the shell is at 80-eV, the inside is at 10-eV, and the fuel is at 2-eV. Also at this time an ion acoustic shock is about to break out of the inside of the shell and enter the fuel. Another feature of great importance at this time is that surface mass flow from the high latitude at 30-degrees towards the equator begins. This flow will ultimately limit the convergence to about 20. As mass flows away from the slide cone, the implosion proceeds more rapidly there, and the final shape of the assembled fuel will be a pancake at the equator. Indeed the choice of a quasi-spherical load to only 30-degrees rather than 45-degrees is made to minimize the effects of this surface mass flow.

From 115- to 121-ns the DT fuel experiences rapid heating to 200-eV as indicated in figure 8. This heating is due to an ion acoustic wave travelling through the fuel towards the center of the shell. At this time, 121-ns, the fuel is slightly over 1-mm in radius, and

the convergence is just under 4. To reach an ignition temperature of 5-keV, a further convergence of 5 is required.

From 121- to 128-ns the fuel is heated to 3.5-keV, and the total convergence is about 20, giving a 400- $\mu\text{m}$ -diameter fuel spot that rapidly distorts to a pancake. The fuel has not reached 5-keV due to some heating of the inner tungsten shell wall. The total width of the tungsten shell is 400- $\mu\text{m}$  at 128-ns. The mean temperature of the tungsten shell at peak compression is 200-eV. For the fuel to reach ignition an additional convergence of 20% would be needed.

The heating of the fuel from 121- to 128-ns is nearly adiabatic as indicated in figure 9, which shows the fuel temperature versus fuel outer radius. For a radius below 0.11-cm the temperature increases as the inverse square of the radius. In this type of load the fuel is heated to roughly 200-eV by an ion acoustic shock, then heated to 3.5-keV by adiabatic compression.

The neutron yield for this load is  $1.5 \times 10^{17}$ . This is a large number for a system that does not even ignite. The energy yield is 400-kJ, which is greater than the kinetic energy drive of 160-kJ. The system could then achieve breakeven with a gain of 2.5. The neutron yield at 127-ns, before the onset of mix while the shell is still imploding with convergence at 13 and temperature at 2-keV, is  $1 \times 10^{15}$ .

## V. Experimental Access

The tungsten shell is of sufficient mass and opacity that radiation from a dopant in the fuel, such as argon, will not be detected when viewed from the outside of the tungsten shell. However such radiation, from argon or neon dopants, can be viewed with the axial diagnostic package on Z through a beryllium window in the glide cone. The axial package supports time-resolved x-ray imaging, spectroscopy, and bolometry for measuring the fuel temperature during the last 10-ns of its compression. The radiation temperature of the inside of the glide cone would also be recorded. The x-ray imaging would record the shell radius as a function of time. For times earlier than 10-ns before peak compression, silicon photodiode arrays or transmission grating spectrometers could be used to measure the fuel temperature.

Side-on x-ray imaging can measure a lower bound for the convergence since the tungsten shell is in general larger in radius than the outer radius of the fuel. Side-on x-ray diagnostics can also record the temperature of the outside of the shell as a function of time, and this would be compared with the LASNEX simulation.

The existing diagnostics are adequate for diagnosing these implosions since the final spot size of any burning fuel would be hundreds of microns.

Neutron activation and time-of-flight detectors are also ready on Z. The neutron time-of-flight detector should receive enough signal to measure ion temperature at bang time.

## VI. High Yield

In order to obtain high yield above 1 GJ, on a machine such as ZX, at 60 MA, a double shell configuration should be used. The outer shell would be made of a high-Z material and filled with DT gas as the main fuel. Inside of the main fuel would be a tungsten spark plug shell filled with igniting fuel. The spark plug is at roughly one-quarter the diameter of the outer shell. As the outer shell compresses the main fuel, plasma pressure builds, implodes the inner tungsten shell, and ignites the fuel in the spark plug. If the burn in the spark plug is strong enough, it will burn through the tungsten shell and ignite the main fuel. This design is very efficient since the main fuel is heated to only 200-eV before it ignites. Such a configuration has ignited the spark plug and burned the main fuel in 1D LASNEX simulations for ZX.

## VII. Summary

2-D LASNEX simulations of the implosion of an 8-mm diameter quasi-spherical tungsten shell on Z filled with 6-atmospheres of DT fuel show the fuel heating to a near-ignition temperature of 3.5-keV with a convergence of 20. The peak implosion velocity is 13-cm/ $\mu$ s. The convergence is limited by surface mass flow from higher latitudes to the equator. As the fuel is compressed to a convergence of 13 the neutron yield is  $1e15$ . The yield of  $1e15$  would be obtained before the onset of mix of the tungsten shell with the DT fuel. The final neutron yield with a convergence of 20 without mix is calculated to be  $1.5e17$ . The DT fuel is heated to 200-eV at a radius of 0.11 cm by an ion acoustic wave. Thereafter the fuel is heated by adiabatic compression to 3.5-keV at a radius of 0.02 cm. The diagnostics in place on Z are adequate to measure convergence, inside and outside shell temperature, and fuel temperature as a function of time.

## References

1. Lindemuth, I.R., and Kirkpatrick, R.C., Nuclear Fusion, **23**, No. 3, 1983
2. F.M. Lehr, A. Alaniz, J. D. Beason, L. C. Carsweee, J. H. Degnan, J. F. Crawford, S.E. Englert, T. J. Englert, J. M. Gahl, J. H. Holmes, T.W. Hussey, G. F. Kiuttu, B.W. Mullins, R.E. Peterkin, N, F. Roderick, P.J. Turchi, and J.D. Graham, J. Appl. Phys., 75 (8), 15 April 1994
3. R. B. Spielman, C. Deeney, G. A. Chandler, M. R. Douglas, D. L. Fehl, M. K. Matzen, D. H. McDaniel, T. J. Nash, J. L. Porter, T. W. L. Sanford, J. F. Seamen, W. A. Stygar, K. W. Struve, S. P. Breeze, J. S. McGurn, J. A. Torres, D. M. Zagar, T. L. Gilliland, D. O. Jobe, J. L. McKenney, R. C. Mock, M. Vargas, T. Wagoner, and D. L. Peterson, Proc. of the 11th Int. Conf. on Particle Beams, edited by K. Jungwirth and J. Ullschmied, Prague, Czech Republic, 1996, p. 150

4. T.J. Nash, M.S. Derzon, G. Allshouse, C. Deeney, J.F. Seaman, J. McGurn, D. Jobe, T. Gilliland, J.J. MacFarlane, P. Wang, and D.L. Petersen , “Dynamic Hohlraum Experiments on SATURN,” Proceedings of the 4th International Conference on High-Density Z-pinches, Vancouver, Canada, p. 175, May, 1997
5. V. P. Smirnov, Plasma Physics and Controlled Fusion, **33**, #13, 1697, 1991
6. J.S. Lash, G. Chandler, G. Cooper, M. Derzon, M. Douglas, D. Hebron, R. Leeper, M. Matzen, T. Mehlhorn, T. Nash, R. Olson, C. Ruiz, S. Slutz, "The Prospects for High Yield ICF with a Z-pinch Driven Dynamic Hohlraum," Proceedings of the 1st IFSA conference, Bordeaux, France, September 1999.
7. Porter, J.L. “Z-pinch driven hohlraums as a radiation source for high energy density physics experiments,” Am. Phys. Soc. **44**, 1948, 1997
8. T.W.L. Sanford, R.E. Olson, R. L. Bowers, G.A. Chandler, M. S. Derzon, D. H. Hebron, R. J. Leeper, R. C. Mock, T. J. Nash, D. L. Peterson, L. E. Ruggles, W. W. Simpson, K. W. Struve, and R. A. Vessey, Phys. Rev. Lett. **83**, 5511, 1999
9. J. Lindl, Phys. Plasmas, **2** (11), November 1995
10. J. D. Huba, NRL Plasma Formulary, 1998

## Distribution

- 1 University of ;New Mexico  
Dept of Chemistry and Nuclear Engineering  
Attn: Prof. G. Cooper  
Albuquerque, NM, 87183
- 5 Los Alamos National Laboratory  
Attn: Darrell Petersen  
Bob Chrien  
Bob Varnum  
George Idzorek  
Bob Watt  
P. O. Box 1663  
Los Alamos, NM 87545
- 2 Naval Research Laboratory  
Attn: J. Davis  
J. Apruzese  
Washington, D.C., 20375
- 1 Cornell University  
Laboratory of Plasma Sciences  
Attn: Prof. D. A. Hammer  
369 Upson Hall  
Ithaca, NY 14853-7501
- 1 MS 1159 Mark Hedemann, 9311  
1 MS 1181 Clint Hall, 1612  
1 MS 1196 Steve Dropinski, 1677  
1 MS 1182 Doug Bloomquist, 1630  
1 MS 1184 Harry Ives, 1639  
1 MS 1186 Steve Slutz, 1674  
1 MS 1186 Tom Mehlhorn, 1674  
1 MS 1186 Joel Lash, 1674  
1 MS 1186 Tom Hail, 1674  
1 MS 1187 Keith Matzen, 1670  
1 MS 1193 Rick Adams, 1673  
1 MS 1193 Dave Hanson, 1673  
1 MS 1187 John McKenney, 16701  
1 MS 1194 Rick Spielman, 1644  
1 MS 1194 Bill Stygar, 1644  
1 MS 1194 John McGurn, 1644  
1 MS 1194 Chris Deeney, 1644  
1 MS 1194 Steve Rosenthal, 1644

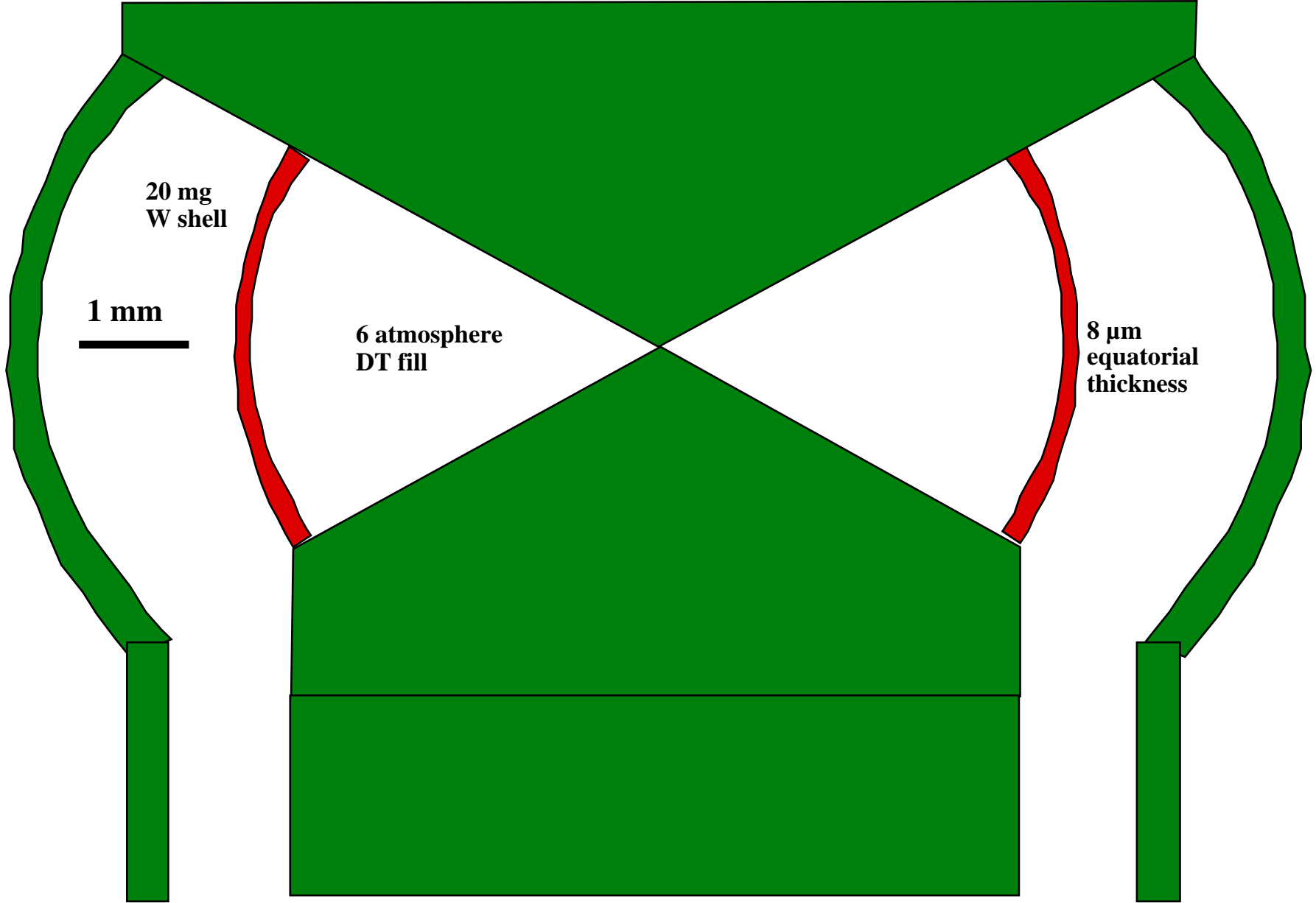


**Figure 1. 8 mm diameter quasi-spherical tungsten load for Z filled with 6 atmospheres of DT fuel.**

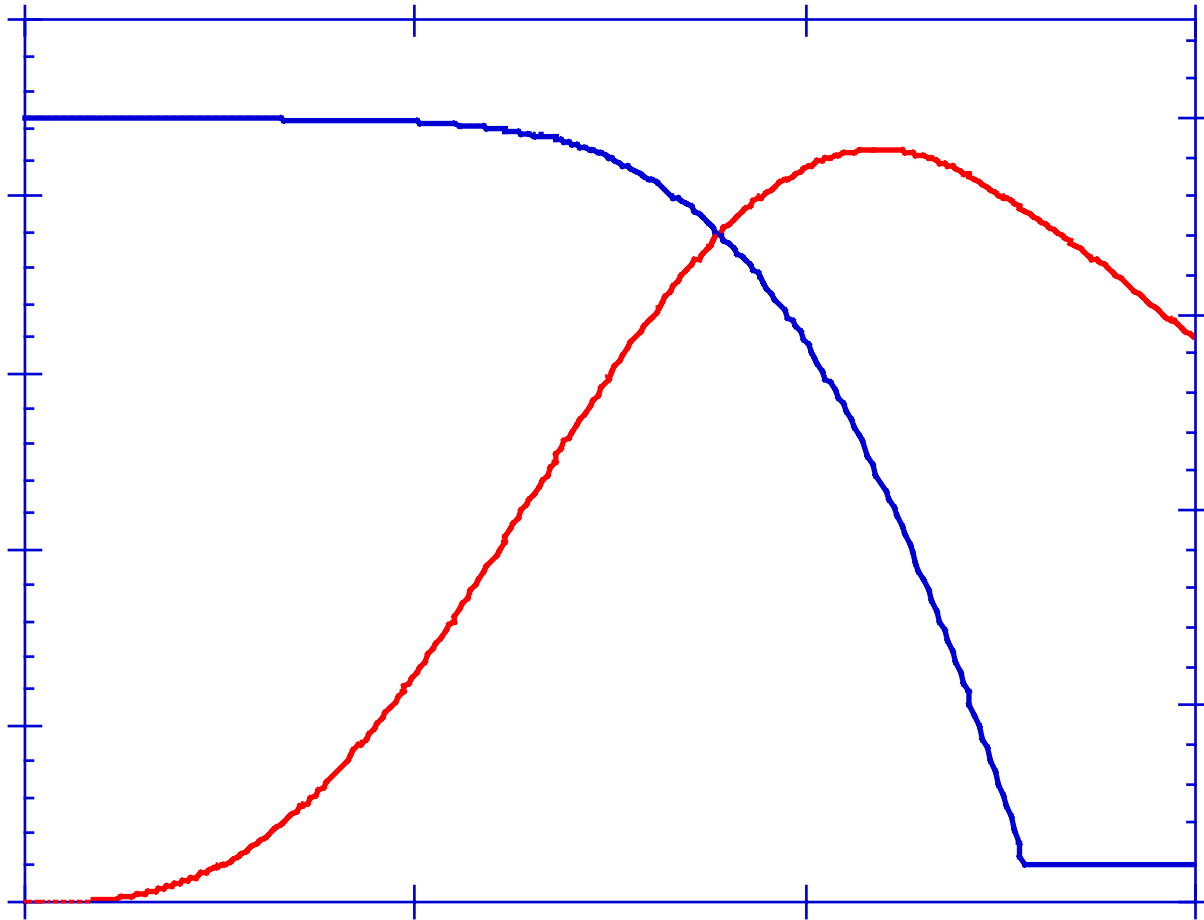


**Figure 2. Radius and current versus time as calculated by SCREAMER for the quasi-spherical load of figure 1.**

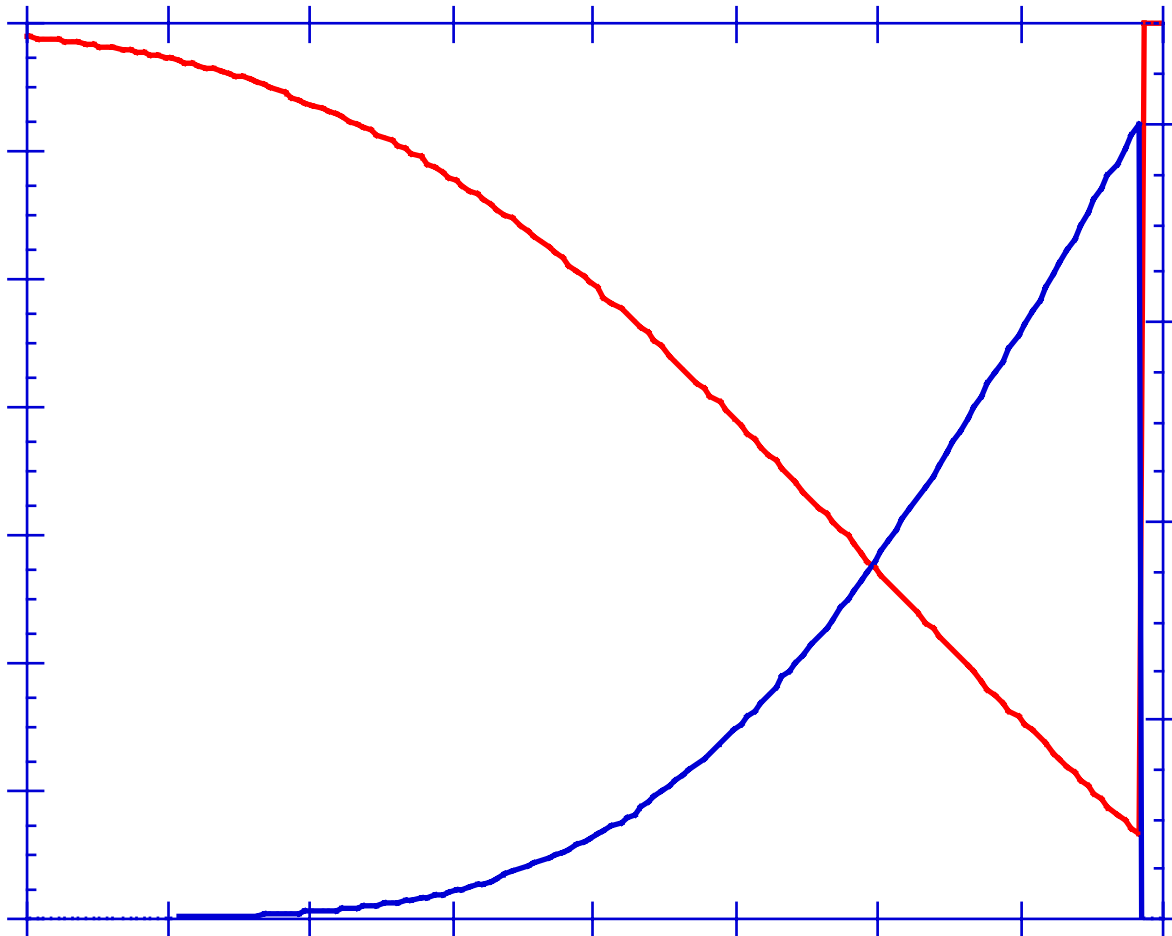


**Figure 3. Velocity and kinetic energy versus time as calculated by SCREAMER for the quasi-spherical load of figure 1.**

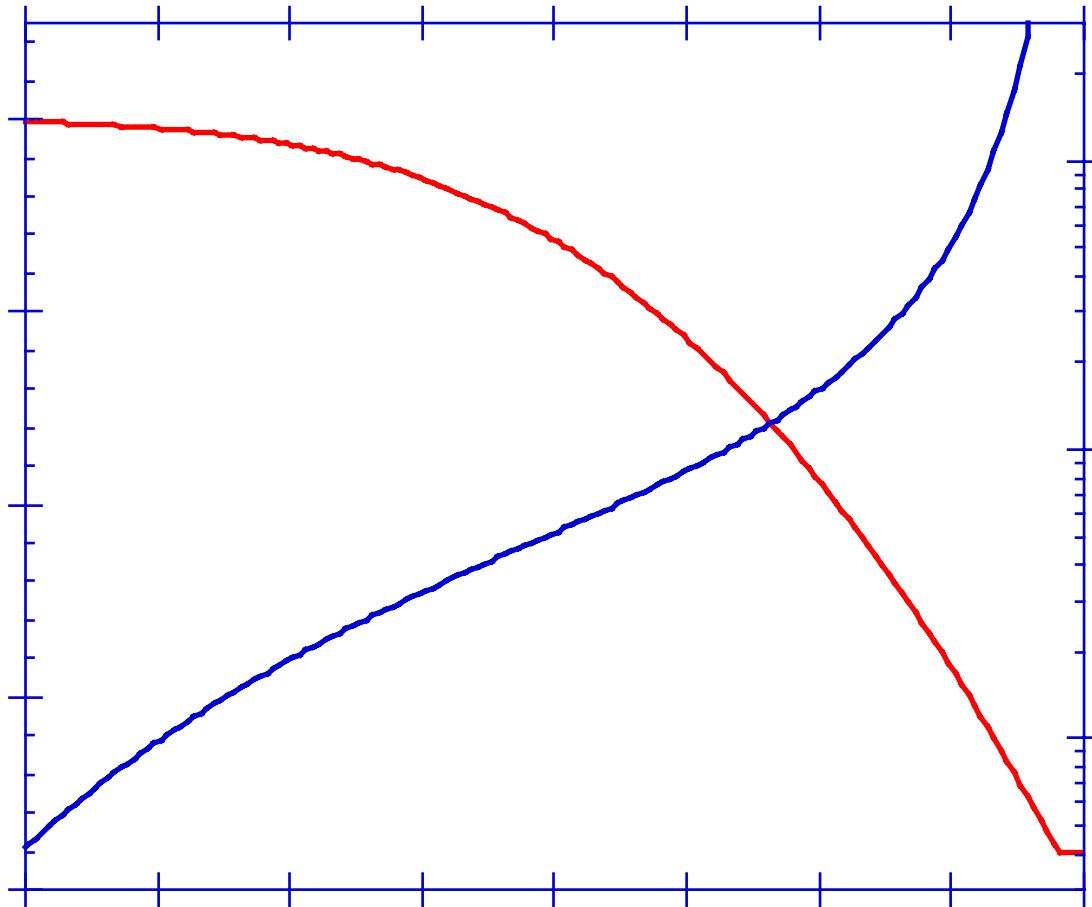


**Figure 4. Radius and magnetic pressure versus time as calculated by SCREAMER for the quasi-spherical load of figure 1.**

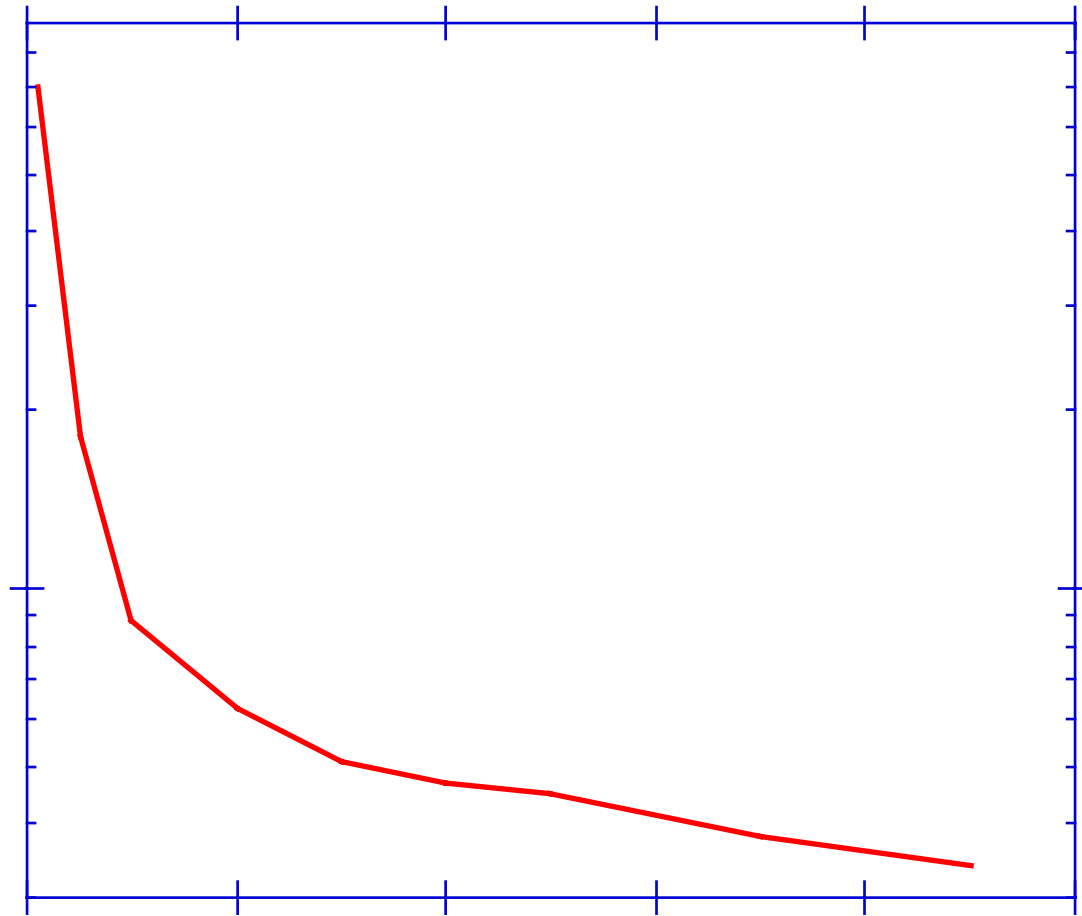


**Figure 5. Skin depth versus plasma temperature for a 100 ns current rise time.**

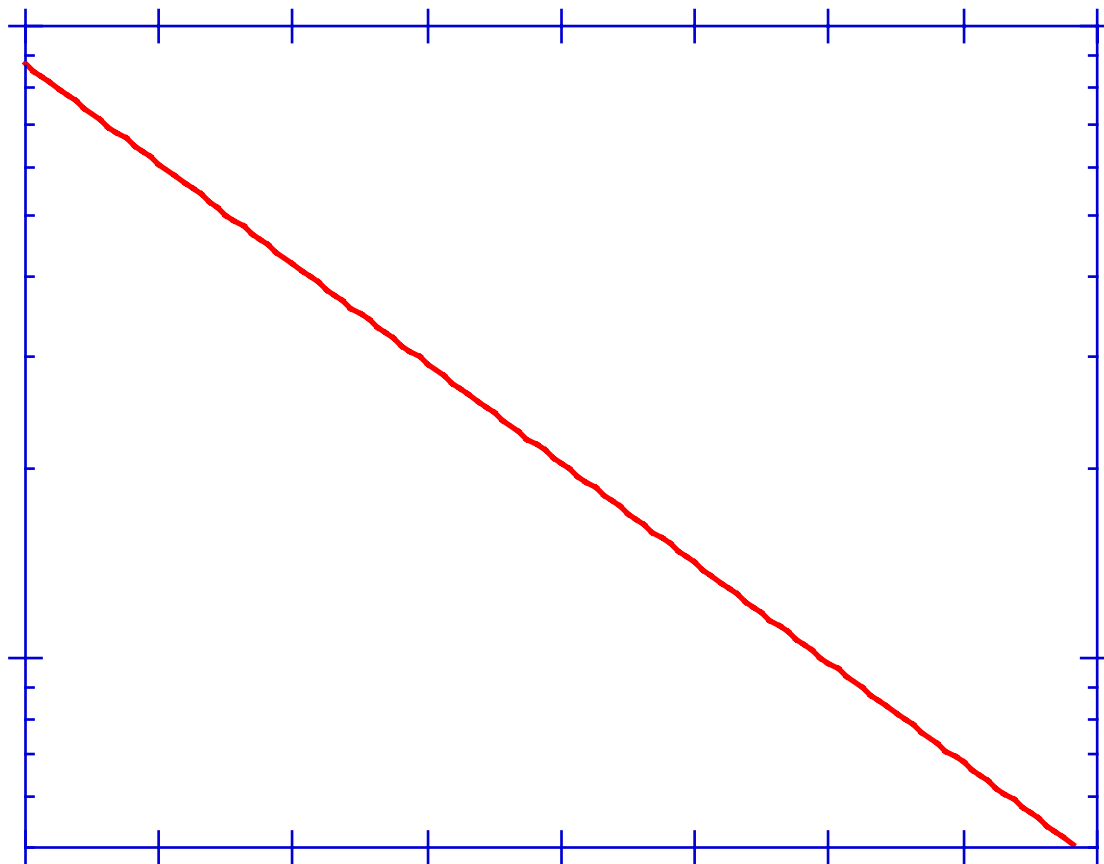


**Figure 6. Temperature variation versus plasma shell depth.**

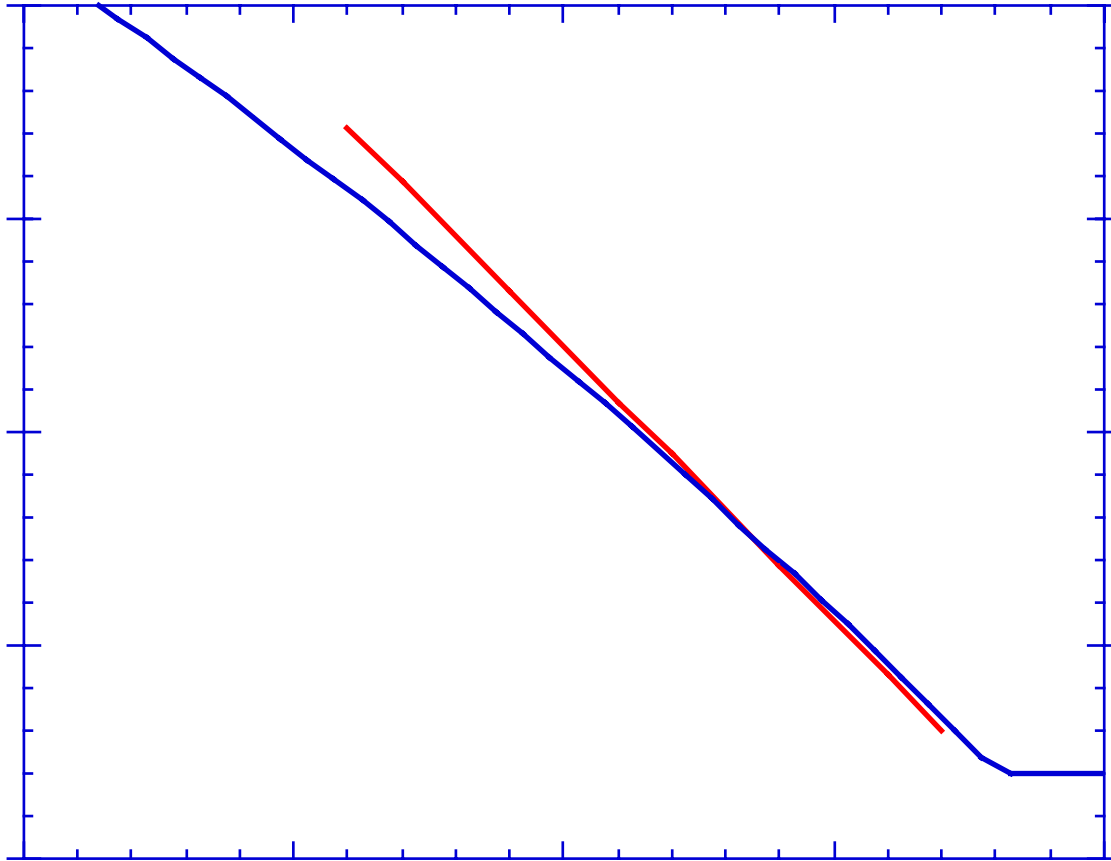


**Figure 7. Radius versus time of imploding shell from SCREAMER and from LASNEX.**

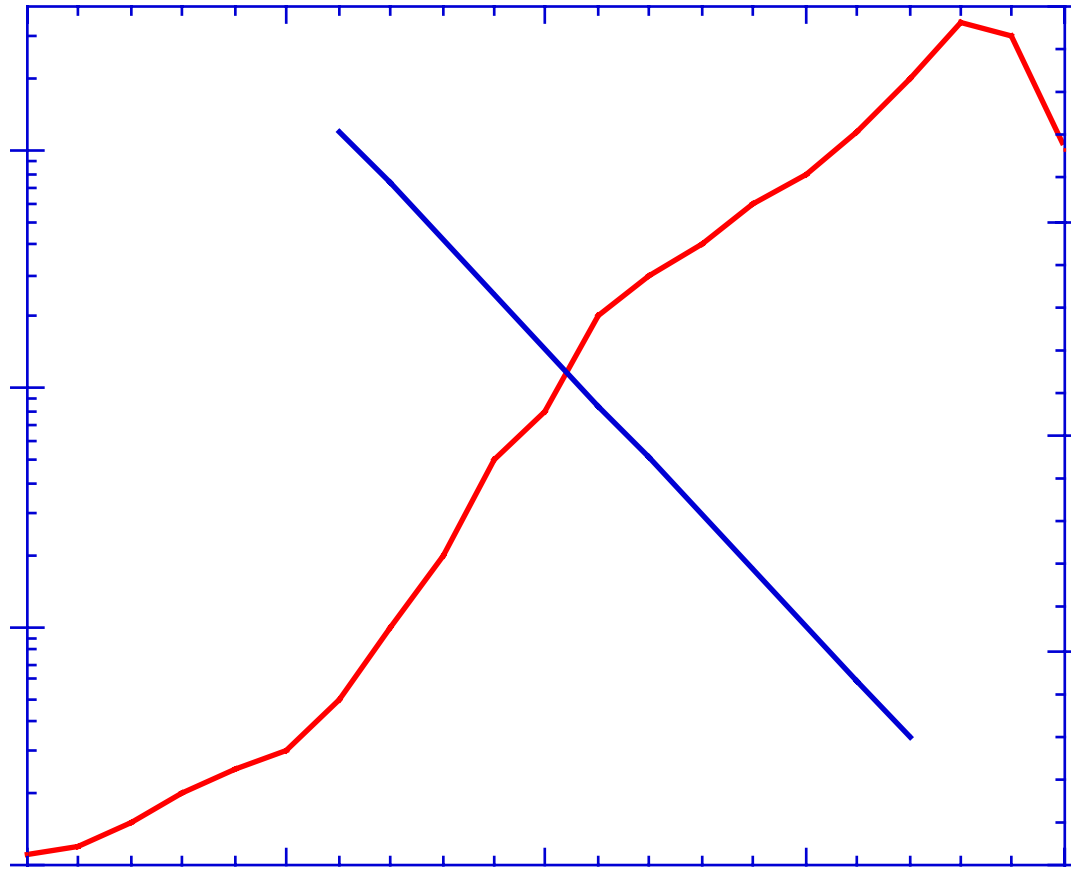


**Figure 8. Fuel temperature and outer radius versus time.**

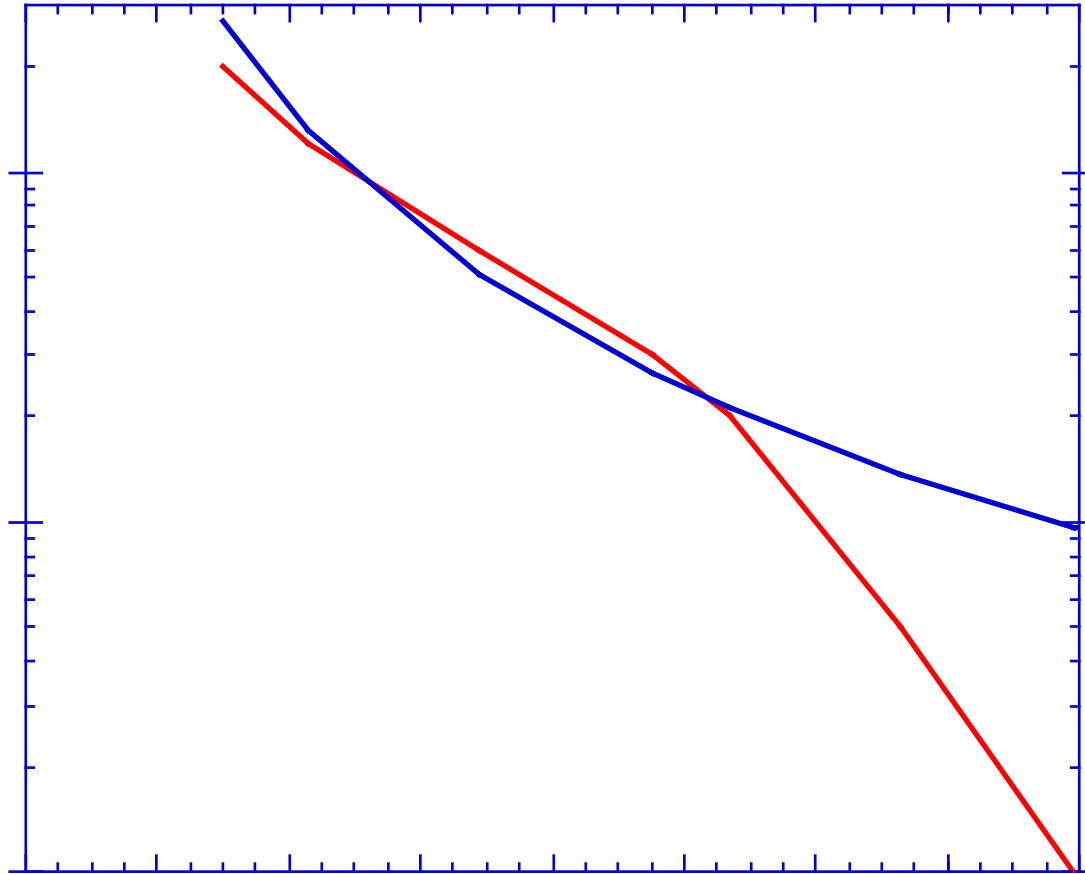


**Figure 9. Fuel temperature versus radius. Below a radius of .11 cm the temperature increases as  $(1/r)^2$ .**

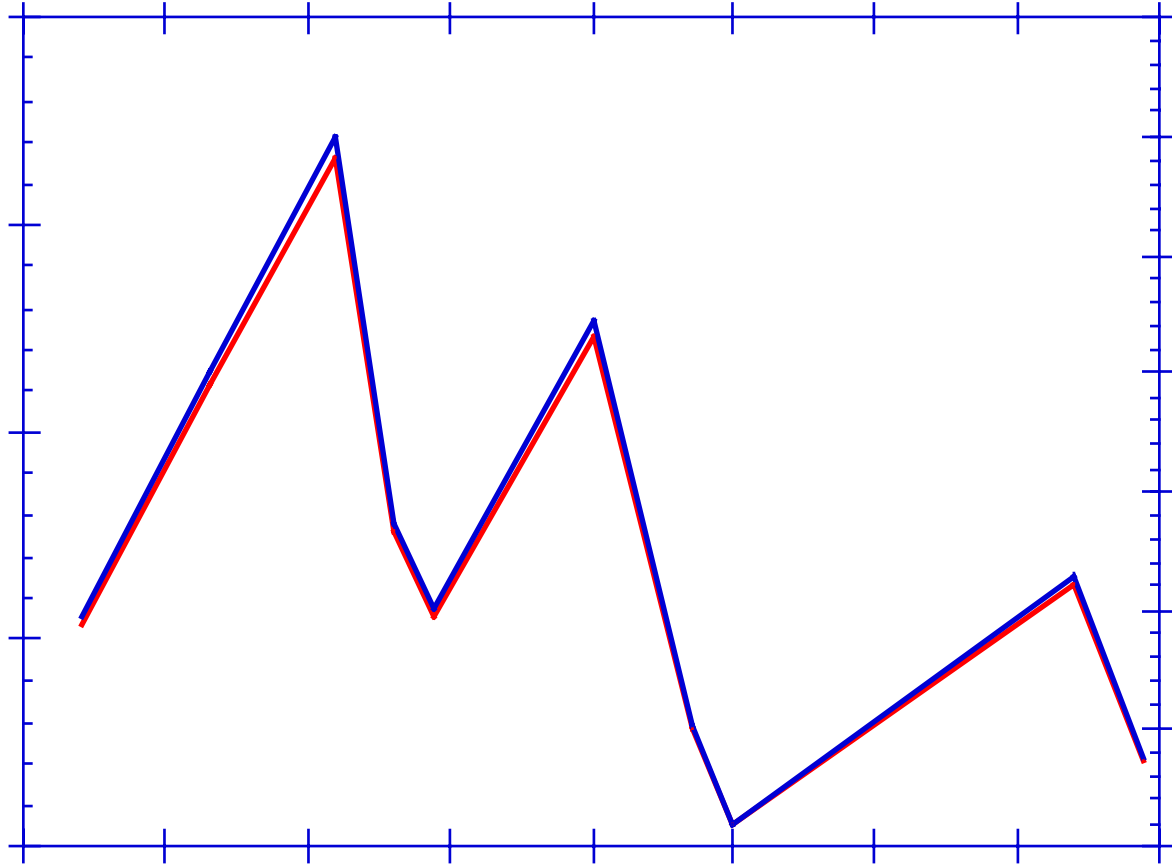


**Figure 10. Maximum fuel to shell mass ratio limited by the shell burst pressure. Titanium shells hold the most fuel.**

1	MS 1194	Dillon McDaniel, 1644
1	MS 1196	Rick Olson, 1677
1	MS 1196	Dave Hebron, 1677
15	MS 1196	Tom Nash, 1677
1	MS 1196	Jim Bailey, 1677
1	MS 1196	Gordon Chandler, 1677
1	MS 1186	Mike Desjarlais, 1674
1	MS 1188	Craig Olson, 1600
1	MS 1193	Guy Bennet, 1673
1	MS 1190	Jeff Quintenz, 1600
1	MS 1191	Mary Ann Sweeney, 1602
1	MS 1159	Christine Coverdale, 9311
1	MS 1178	Roy Hamil, 1612
1	MS 1181	Jim Asay, 1675
1	MS 1181	Marcus Knudson, 1675
1	MS 1186	Tim Pointon, 1674
1	MS 1186	Barry Marder, 1674
1	MS 1186	Peter Stoltz, 1674
1	MS 1186	Roger Vesey, 1674
1	MS 1193	John Porter, 1673
1	MS 1193	Mike Cuneo, 1673
1	MS 1187	Dan Jobe, 16701
1	MS 1187	Dan Nielsen, 16701
1	MS 1192	Jim Potter, 1636
1	MS 1192	Jerry Mills, 1636
1	MS 1194	Mike Mazarakis, 1644
1	MS 1194	Ken Struve, 1644
1	MS 1194	Melissa Douglas, 1644
1	MS 1194	Tim Wagoner, 1644
1	MS 1196	Ray Leeper, 1677
1	MS 1196	Al Schmidlapp, 1677
1	MS 1196	Jose Torres, 1677
1	MS 1196	Carlos Ruiz, 1677
1	MS 1196	Tom Sanford, 1677
1	MS 1193	Steve Lazier, 1673
1	MS 1194	Dave Lepell, 1644
1	MS 9018	Central Technical Files, 8945-1
2	MS 0899	Technical Library, 9616
1	MS 0612	Review and Approval Desk for DOE/OSTI, 9612